Response to Referee #1 comments

We thank the referee for the careful reading of our manuscript and the constructive comments, which helped us to substantially improve the clarity and depth of the work. Below, we reply to each comment point by point.

Comment 1

In "Settings", elaborate on the age of sediments: you use the names of Holocene Lacustrine sediments and glaciolacustrine deposits. But glaciolacustrine deposits are also of Holocene age, right? In a few sentences, address the age of the sediments and then tell which nomenclature you are using through the whole manuscript. Also, at some point you refer to "Holocene sub-basins on the slopes and glaciolacustrine sub-basins" – how were these assigned?

We agree that this needed clarification. The glaciolacustrine deposits were emplaced during the deglaciation of the area and are thus of latest Pleistocene age, predating Unit 3, which in south-Chilean piedmont lakes comprises diatomaceous lacustrine sediments accumulated since ~17 ka (Bertrand et al., 2008; Heirman, 2011; Van Daele et al., 2016). We consequently replaced the age-based label "Holocene lacustrine sediments" with "diatomaceous lacustrine sediments (Unit 3)" throughout the manuscript, while retaining "glaciolacustrine deposits" for the underlying, more clastic Unit 2. The age framework and the nomenclature are now revised explicitly in the Setting. The sub-basins in Figure 2 were assigned from the ponded, onlapping infill geometries of the corresponding seismic-stratigraphic units within local depressions; this is now revised in the figure caption.

Changes in the manuscript:

> **Section 2 (Setting):** *"In south-Chilean piedmont lakes, the uppermost of these units comprises diatomaceous lacustrine sediments that have accumulated since the deglaciation at ~17 ka (Bertrand et al., 2008; Heirman, 2011; Van Daele et al., 2016), whereas the underlying glaciolacustrine deposits were emplaced during deglaciation itself and are thus of latest Pleistocene age. Throughout this manuscript we use the seismic-stratigraphic nomenclature (Units 0-3; Section 3.1.1), with the lithological terms (diatomaceous lacustrine sediments, glaciolacustrine deposits, glacial till, bedrock) serving as descriptive labels for these units."*
>
> **We have modified the caption of Figure 2:** *"Blue and orange arrows delineate Holocene sub-basins on the slopes and glaciolacustrine sub-basins, respectively, assigned based on the ponded, onlapping infill geometries of the corresponding seismic-stratigraphic units within local depressions."*

Comment 2

Have you validated sediment properties (vp, vs, density) from the literature by measurements on the samples? What are the uncertainties and did you do any sensitivity analysis of the influence of uncertainties on the modelling results? If not, how would you expect them to influence the result and how big uncertainties do you expect? Please add this (and how one could address these uncertainties) in the Discussion of other parts of the text. Did you also need to include some damping/quality factors or other sediment parameters into the model?

We thank the referee for raising this point and have now addressed it on three levels in the manuscript: which properties are measured versus adopted, the uncertainty bounds on the adopted velocities, and how that uncertainty propagates to the results.

Bulk density is measured on the studied, unopened cores (0.5 cm resolution Geotek Multi-Sensor Core Logger; Molenaar et al., 2021). Lake core Vp logs were acquired on the same cores, but they cover only the uppermost meters of Unit 3 and do not constrain the deeper depth and units, which dominate the impedance structure; no Vs measurements exist for the lake yet. The model velocities were therefore adopted from published analogues, with the reported literature range of each unit treated as its uncertainty. Material damping is included as 5% Rayleigh damping anchored at 0.5 and 10 Hz, now revised in Section 3.3.1.

The propagation of these uncertainties is addressed by (i) the stepwise BM02-BM07 and flat-layer models, which have property variations larger than the plausible range of any single unit while preserving the spatial pattern and the exceedance of the GMPE predictions, (ii) the alternative-Vp model (Comment 3), and (iii) new elastoplastic sensitivity runs (new supplements). These points, and how the uncertainties could be reduced by future in-situ measurements, are added in the new Section 5.5.

Changes in the manuscript:

> **Section 3.1.2:** *"Of the model parameters, bulk density is directly constrained by measurements on the studied (unopened) sediment cores (Section 3.3.1), and available whole-core Vp logs cover only the uppermost meters of Unit 3, whereas no Vs measurements exist for Lake Riñihue; the model velocities of all units were therefore adopted from the analogues and empirical relationships above. We treat the reported literature range of each unit as the uncertainty on the adopted value; the propagation of these velocity uncertainties to the simulated ground motions is addressed by the stepwise property substitutions of Section 3.3.1 and discussed in Section 5.5."*

Section 3.3.1: *"...material damping is represented by Rayleigh damping with a target ratio of 5%, anchored at 0.5 and 10 Hz to bracket the basin fundamental frequencies and the dominant input frequencies."*

New Section 5.5 (fourth paragraph): *"Apart from lake core Vp logs restricted to the uppermost meters of Unit 3 (Section 3.1.2), no velocity measurements exist for Lake Riñihue: the model velocities were adopted from analogue settings and empirical relationships, so the associated literature ranges represent a uncertainty on the absolute amplification. The stepwise unit models (BM02-BM07 and the flat-layer models) impose property variations larger than the plausible uncertainty of any individual unit and preserve both the spatial response pattern and the exceedance of the GMPE predictions, while the alternative Vp model (Table S1; Figures S2-S3) yields a similar pattern with ~30% higher absolute amplitudes. The preferred, consolidated Vp setting is thus conservative with respect to this parameter choice (i.e., it yields the lower of the two amplification estimates), within the linear framework that itself constitutes an upper bound. Future in-situ shear-wave measurements and laboratory characterization of the dynamic properties of these lacustrine units would reduce these uncertainties most directly."*

Comment 3

You used two Vp settings (L.146-151), what was their impact and which one do you trust more? How was it included in different models (Table 2)? Address the difference in the outcome of 2D numerical simulations using both models. Why are there no alternative models for Vs, for example?

The alternative Vp setting (1800 m s-1, unconsolidated glaciolacustrine deposits) was propagated through all seven parameter sets of Table 2, isolating the compressional-stiffness uncertainty of Unit 2. It yields ~30% higher absolute ground motions (PGA locally ~2 g vs. ~1.5 g for the 1960 event) with similar spatial patterns and conclusions (Figures S2-S3). We consider the consolidated setting (2200 m s-1) more plausible and note that it yields the lower of the two amplification estimates, so our main result is conservative with respect to this choice.

Regarding Vs: the BM02-BM07 and flat-layer substitutions already impose Vs variations far larger than the plausible range of any individual unit and thus function as an effective Vs sensitivity test, and the adopted Vs values are independently constrained (Caiti et al., 1994; Carr et al., 1998; Shynkarenko et al., 2021). We agree that dedicated Vs perturbation runs could also have been explored; this is noted as a limitation in Section 5.5.

Changes in the manuscript:

Section 3.1.2: *"This alternative setting yields ~30% higher absolute ground motions with an identical spatial pattern (Figures S2-S3), so that the preferred, consolidated setting is conservative with respect to this parameter choice (Section 5.5)."*

New Section 5.5 (fourth paragraph): see the text quoted under Comment 2, which covers the Vs sensitivity provided by the BM02-BM07 and flat-layer models and the alternative-Vp test.

Comment 4

Add to the discussion or where suitable, how the properties of investigated lake sediments are expected to influence its seismic response. Does it correspond to what you obtained from the modelling?

The response is expected to be governed by (i) the strong impedance contrasts between the soft lake sediments and the progressively stiffer underlying units, (ii) the stacking of distinct units across which amplification accumulates, and (iii) the low-density, high-porosity, diatom-rich nature of the lacustrine sediments themselves (Wiemer and Kopf, 2017; Wiemer et al., 2017), which makes them both highly amplifying and susceptible to nonlinear softening and excess pore-pressure generation under strong shaking. The modeling reproduces (i) and (ii): the realistic model (BM01), retaining the full succession of contrasts, yields the strongest amplification; stepwise replacement of deeper units (BM01 to BM03) reduces it; and removing only the Holocene cover (BM04) reduces it by ~15-25%. Influence (iii) is addressed by the new elastoplastic sensitivity runs supplements, while pore-pressure effects, which the total-stress PIMY model cannot represent, are now explicitly discussed as a limitation. This discussion is added in Sections 5.1 and 5.5.

Changes in the manuscript:

Section 5.1 (new paragraph): *"The seismic response of these sediments is thus expected to be governed by (i) the strong impedance contrasts between the soft lake sediments and the progressively stiffer underlying units, (ii) the stacking of distinct units across which amplification accumulates, and (iii) the low-density, diatom-rich nature of the sediments themselves (Wiemer and Kopf, 2017; Wiemer et al., 2017), which makes them prone to nonlinear softening and pore-pressure generation under strong shaking. The simulations reproduce the first two expectations, as shown by the stepwise model comparisons below, whereas the third is only partly captured, through the elastoplastic sensitivity runs, and is further discussed in Section 5.5."*

Section 5.1 (revised sentence): "*Despite the relatively high static shear strength imparted by particle interlocking of diatom frustules, diatomaceous sediments are prone to developing excess pore water pressure and potential liquefaction under cyclic seismic loading (Wiemer and Kopf, 2017; Wiemer et al., 2017),* *processes that the present total-stress simulations cannot capture (Section 5.5).”*

Section 4.3.2: *“However, the highest ground motions among all BMs are still achieved by BM01, as it is the only model that retains the full succession of impedance contrasts of the real stratigraphy, so that wave energy is trapped at several successive interfaces.”*

New Section 5.5 (second paragraph): *“The PIMY model is a total-stress, pressure-independent formulation and does not simulate the generation and dissipation of excess pore-water pressure. Diatomaceous sediments are prone to developing excess pore pressure and potential liquefaction under cyclic loading (Wiemer and Kopf, 2017; Wiemer et al., 2017), processes that may locally modify both the amplification and the sediment deformation and that constitute a target for future effective-stress modeling.”*

Comment 5

182: address how nonlinear site amplifications can influence observed seismic impact in comparison to linear case. Are there magnitude/distance thresholds at which you expect switch from linear case to non-linear? Or how is this distinction used?

In the GMPEs, the linear/nonlinear distinction is an intrinsic feature of the site term: below a reference velocity (Vlin = 865.1 m s-1 for PGA; Vref = 725 m s-1 for PGV), the predicted site amplification decreases with increasing bedrock-site ground motion, i.e., stronger input shaking yields proportionally less amplification. The transition is continuous, so there is no discrete magnitude or distance threshold; magnitude and distance enter only indirectly through the predicted bedrock-site motion. All Lake Riñihue sites (Vs30 of ~100-450 m s-1) lie below these reference velocities and are therefore consistently evaluated with the nonlinear site term, with a stronger reduction for the 1960 event (basement PGA of ~0.5 g) than for 2010 (~0.2 g). We further note that the softest lake sites (~100 m s-1) fall below the stated validity range of the PGV site term (200-1000 m s-1), implying extrapolation. These clarification has been added to Section 3.2, and this extrapolation is listed in Section 5.5. In our 2D simulations, the main analysis is linear visco-elastic and nonlinearity is examined separately in the Supplement (Comment 18).

Changes in the manuscript:

Section 3.2: *“In both models the site term is nonlinear for soft sites: below a reference velocity (Vlin = 865.1 m s-1 for PGA, Montalva et al., 2017; Vref = 725 m s-1 for PGV, Montalva et al., 2022), the predicted site amplification decreases with increasing bedrock-site ground motion, i.e., stronger input shaking yields proportionally less amplification. As all Vs30 values in Lake Riñihue (~100-450 m s-1) lie well below these reference velocities, the site terms are consistently evaluated in their nonlinear branch for both events, and the lowest values (~100 m s-1) fall below the stated validity range of the PGV site term (200-1000 m s-1; Montalva et al., 2022), implying extrapolation for the softest lake sites (Section 5.5).”*

New Section 5.5 (in final paragraph): *“Two limitations concern the empirical reference. The Mw 9.5 magnitude of the 1960 event exceeds the calibration range of the considered GMPEs (unlike the 2010 Mw 8.8 Maule event, which is part of their calibration dataset), and Vs30 values in the lake interior (down to ~100 m s-1) fall below the validity range of the PGV site term (Montalva et al., 2022), so the GMPE reference estimates and the derived target spectra involve extrapolation.”*

Comment 6

What are the limitations of 2D modeling you used (e.g., in comparison to 3D)? Address in Discussion.

We agree that these limitations should be addressed and have added them to the new Section 5.5: the neglect of out-of-plane propagation, 3D focusing and 3D basin resonance (for which literature indicates that 2D sections tend to underestimate amplification in three-dimensionally confined depressions, making our results conservative in this respect), and the assumption of vertically incident, in-plane SV waves. We also clarify that the profile was deliberately oriented parallel to the subbasin axis to minimize out-of-plane effects.

Changes in the manuscript:

New Section 5.5 (third paragraph): *“The 2D approach neglects out-of-plane wave propagation, three-dimensional focusing and 3D basin resonance; previous comparisons indicate that 2D cross-sections tend to underestimate the amplification of three-dimensionally confined depressions (e.g., Parla and Somala, 2022), so our results are conservative in this respect. The simulations further assume vertically incident, in-plane SV waves, neglecting oblique incidence, additional wave types and rupture directivity. The modeled profile was oriented parallel to the subbasin axis to minimize out-of-plane geometric effects, and future 3D simulations would require a three-dimensional velocity model of the full basin and substantially larger computational resources.”*

Comment 7

Modelling: how did you chose the "pressure-independent multi-yield plasticity (PIMY) model"? Did you consider *other constitutive models?*

This comment prompted us to make the use of the constitutive model explicit: the main results use the linear visco-elastic response of the PIMY model (materials kept at their initial elastic stage), while the fully elastoplastic PIMY response is provided as a supplementary sensitivity analysis. Using the same model for both cases means the linear and nonlinear analyses share an identical formulation and mesh, so differences are attributable to hysteretic behavior alone. PIMY suits the fine-grained, cohesive deposits of Units 3 and 2, whose undrained cyclic strength is essentially independent of confining pressure. We considered but did not adopt pressure-dependent multi-yield models (PDMY), formulated for cohesionless, liquefiable sands and requiring dilatancy and pore-pressure calibration unsupported by available data, and equivalent-linear approaches, which are effectively one-dimensional and cannot represent the 2D wave propagation central to this study.

Changes in the manuscript:

> **Section 3.3.1 (new paragraphs):** *"In the main analysis, the PIMY materials are kept in their initial, linear elastic stage, and material damping is represented by Rayleigh damping with a target ratio of 5%, anchored at 0.5 and 10 Hz to bracket the basin fundamental frequencies and the dominant input frequencies; the main simulations are thus linear visco-elastic, isolating the impedance- and basin-geometry effects that are the focus of this study. The fully nonlinear (elastoplastic) PIMY response is evaluated separately as a sensitivity analysis in the Supplement (Figures S14-S15), and its implications are discussed in Section 5.5."*
>
> *"…… PIMY was adopted because the fine-grained, cohesive lacustrine deposits of Units 3 and 2 exhibit an undrained cyclic strength that is essentially independent of confining pressure (e.g., Kramer, 1996; Yang et al., 2003), which is the behavior represented by its von Mises-type, pressure-independent yield surfaces, and because keeping the same model at its elastic stage allows the linear and nonlinear analyses to share an identical formulation and mesh. Pressure-dependent multi-yield models (PDMY), formulated for cohesionless, potentially liquefiable sands, and equivalent-linear approaches, which are effectively one-dimensional and cannot represent the 2D wave propagation central to this study, were considered but not adopted. Note that PIMY is a total-stress formulation and does not simulate the generation of excess pore-water pressure (Section 5.5)."*

Comment 8

261-262: "recording sites with Vs30 > 700 m s-1 to represent basement conditions" – why did you choose vs30>700 m/s as a criterion for basement? Provide a reference for such a decision. Why not using the records from the sites/depths with Vs>800 m/s (engineering bedrock)?

The threshold approximates the implicit reference condition of the target spectra, which are computed without the site term: the PGA model uses Vlin = 865.1 m s-1 and the PGV model Vref = 725 m s-1, so no single Vs30 corresponds to both. Vs30 > 700 m s-1 is a practical lower bound near the NEHRP B/C boundary (760 m s-1; BSSC, 2003) and below both model reference velocities. A stricter 800 m s-1 criterion would remove two of the seven records used for the 1960 input and one for 2010, leaving too few megathrust recordings in the target magnitude range; moreover, all records are spectrally matched to the same basement reference target, so the residual stiffness difference has a minor effect on the matched inputs. The rationale and reference are now given in Section 3.3.2.

Changes in the manuscript:

> **Section 3.3.2:** *"This threshold lies near the NEHRP B/C site-class boundary (760 m s-1; BSSC, 2003) and below the reference velocities of the site terms of both GMPEs (Vlin = 865.1 m s-1 for PGA; Vref = 725 m s-1 for PGV), ensuring that the selected records approximate the stiff reference-site condition of the target spectra while retaining a sufficient number of megathrust recordings in the target magnitude range."*

Comment 9

Section 3.4, L. 279-280: could you show seismic profile/core photos illustrating what you mean by "surficial sediment remobilization (SSR) and soft-sediment deformation structures (SSDS)" and discuss how you identify them?

SSR is identified as centimeter scale stratigraphic gaps through high-resolution multi-proxy correlation of slope cores against the continuous reference sequence of the flat basin interior (e.g., core CRIN8; Figure 8e). SSDS are identified on CT images as in-situ deformation of originally horizontal laminations, classified into the three types related to Kelvin-Helmholtz instability following Molenaar et al. (2021, 2022). While SSDS can locally be visible on high-resolution seismic data, their thickness and type cannot be assessed at the seismic vertical resolution (~10-20 cm for the pinger), so both imprint types are identified and quantified on the cores. CT scans of cores were already provided (Figures 8c-e and S4), but Section 3.4 did not define the imprints or point to these figures; both are now added.

Changes in the manuscript:

> **Section 3.4:** *"...surficial sediment remobilization (SSR), i.e., the coseismic erosion of a thin, centimeter scale veneer of surficial sediment on the lacustrine slopes (Moernaut et al., 2017; Molenaar et al., 2021), and soft-sediment deformation structures (SSDS), i.e., in-situ deformation of originally horizontal laminations resulting*

from shear-induced Kelvin-Helmholtz instability at density interfaces (Heifetz et al., 2005; Molenaar et al., 2022). Both imprint types (~1-25 cm) are identified and quantified on medical CT scans of the cores, where the density contrast of individual laminations allows sub-centimeter characterization of their thickness and type (Figures 8c-e and S4).”

Comment 10

You use Kriging to interpolate sediment properties. Which Kriging algorithm do you use specifically? Add name and reference(s).

We thank the reviewer for pointing this out, we indeed forgot to specify this in the manuscript. The depth-converted horizon picks were interpolated using point ordinary kriging with a linear variogram model; the algorithm and references are now given in Section 3.1.2.

Changes in the manuscript:

Section 3.1.2: *“...and then the converted depth horizons were spatially interpolated using point ordinary kriging with a linear variogram model (e.g., Cressie, 1990; Oliver and Webster, 1990) to generate continuous surfaces across the lake basin.”*

Comment 11

Sediment cores you mention in the study (in particular, in Fig. 4 and section 4.4.1) – how deep are they? Is their full length shown in Fig. S4? Could they be used to validate the properties of your model and properties interpolation? Could you provide a summary of core depths and events identified in them in the manuscript? Either as a table or a map where maybe depth can be shown with color and event type with symbol shape.

The studied cores are short gravity cores (1-2 m long). They provide a direct check on the shallowest model parameters, e.g., bulk density (Molenaar et al., 2021), but the deeper part of Unit 3 and all underlying units are beyond their reach and cannot be validated by core data; those properties and the interpolated horizon geometries rest on the seismic-reflection data and published analogues (Comment 2). Figure S4 intentionally shows only the correlated interval around the 1960 event horizon, which is the interval relevant for the imprints. As suggested, we have added a new supplementary table (Table S4) summarizing, for each core, the water depth, slope angle, and the 1960 imprints (SSR depth; SSDS thickness and type), and we clarified the core lengths in Section 3.4. The new table is reproduced below as Table R1.

Table R1. Summary of the studied sediment cores and their sedimentary imprints attributed to the 1960 Mw 9.5 Valdivia earthquake (to be included in the Supplement as Table S4)

Core ID	Water depth (m)	Slope angle (°)	SSR depth (cm)	SSDS thickness (cm)	SSDS type	Total imprint thickness (cm)
RIN17-01	64	5.7	20	-	-	20
RIN17-02	64	5.7	20	-	-	20
RIN17-03	88	3.3	-	3	Disturbed lamination	3
RIN17-04	82	2.8	-	4	Folds	4
RIN17-05	58	2	5	3	Folds	8
RIN17-06	39	3.7	5	7	Folds	12
RIN17-07	74	1.9	1	5	Disturbed lamination	6
RIN17-08	96	2.6	5	5	Disturbed lamination	10
RIN17-09	83	8	1	5	Folds	6
RIN17-10	60	8.7	6	8	Folds	14
RIN17-11	86	2	1	25	Folds	26
RIN17-12	105	3.1	4	-	-	4
RIN17-14	113	0.5	-	-	-	0
RIN17-17	110	0.9	4	-	-	4
RIN17-18	68	2.4	6	1	Disturbed lamination	7
RIN17-19	63	6.3	2	4	Folds	6
CRIN8	113	0.5	-	-	-	0
CRIN10	189	1	-	-	-	0
CRIN12	79	1.8	6	-	-	6

Changes in the manuscript:

Section 3.4: *“The studied cores are short gravity cores (1-2 m long) that sample only the uppermost part of Unit 3; the deeper units are beyond their reach, so the cores constrain the shallowest model parameters (e.g.,* *bulk density; Section 3.3.1) but cannot be used to validate the velocities of the deeper units. A summary of the water depth, slope angle and identified 1960 imprints of each core is given in Table S4."*

Comment 12

Why do you have higher PGA at sites with thinner and stiffer sediments? This needs an explanation. Is this due to damping of energy at high frequencies by soft sediments? Can this also be the effect of non-linearity?

Both mechanisms contribute. At the thin, stiff western margin, site amplification occurs at relatively high frequencies, the band that controls PGA, whereas in the thick, soft eastern sediments high-frequency energy is dissipated by material damping while longer-period energy is amplified, lowering PGA but raising PGV. In the GMPE predictions, the nonlinear site term additionally reduces the predicted PGA at the softest sites; in the 2D simulations, the elastoplastic sensitivity runs show the equivalent effect (Comment 18). An explanatory sentence has been added to Section 4.2.

Changes in the manuscript:

> **Section 4.2:** *"Conversely, PGA is controlled by high-frequency motion, which is preferentially amplified at the stiffer, thinner-sediment sites along the western margin, whereas in the thick, soft eastern sediments high-frequency energy is dissipated and the nonlinear site term of the GMPEs further reduces the predicted PGA (Section 3.2)."*

Comment 13

372 "the highest ground motions among all BMs are still achieved by BM01" – address why this is the case.

BM01 is the only model retaining the full sequence of impedance contrasts of the real stratigraphy, so constructive trapping of wave energy occurs at several successive interfaces, with the softest surface unit providing the largest contrast at the shallowest interface. Each modified model removes or weakens at least one contrast (BM02-BM03 the deeper ones, BM04 the soft surface layer, BM05 the deepest till-bedrock contrast), reducing the cumulative amplification. This is now revised in Section 4.3.2 and elaborated in Section 5.1.

Changes in the manuscript:

> **Section 4.3.2:** *"However, the highest ground motions among all BMs are still achieved by BM01, as it is the only model that retains the full succession of impedance contrasts of the real stratigraphy, so that wave energy is trapped at several successive interfaces."*

Comment 14

You mentioned several times contrasts in sediment properties. Address their influence on the amplification in the discussion. Section 4.3.2: BM05 shows quite a flat amplification. Does it mean that the contract between Unit 0 and 1 has the strongest impact on the amplification? BM03 includes the highest acoustic impedance contrast among all the models. Interestingly, the amplification is not that high but you see localized peaks on the slope. Do you have an idea why?

Across BM01-BM05 the overall amplification scales with the number of impedance contrasts retained. In BM05, weakening the deepest (till-bedrock) contrast indeed produces the largest single reduction, because this interface controls how much upward-incident energy is reflected back into the overlying units; this is now revised in Section 4.3.2. In BM03, a single strong shallow contrast reflects a large fraction of the incident energy back into the bedrock, lowering the overall level, while the same strong, shallow contrast makes basin-edge-generated surface waves more efficient, so the sub-basin geometry produces pronounced localized slope peaks. That these peaks are geometry-controlled is compared to the flat-layer models with identical properties (Figures S5-S8), which reproduce the amplification level but not the peaks.

Changes in the manuscript:

> **Section 4.3.2:** *"BM05 (Figures 6e and 7e), in which the basement is replaced by till properties, leads to the largest reduction in ground motion strength among the single-unit substitutions (~50%), indicating that the deepest (till-bedrock) contrast is the single largest contributor to the overall amplification, as it controls how much of the upward-incident energy is reflected back into the overlying units."*
>
> **Section 4.3.2:** *"...yet PGA and PGV further show more prominent localized peaks on the slopes: the strong, shallow contrast between the low-velocity Unit 3 and the underlying bedrock makes the surface waves generated at the sub-basin edges more efficient, so that the geometry-controlled slope peaks become more pronounced even as the overall amplification level decreases."*

Comment 15

How does the observed amplification in the lake compare with the amplifications expected in the literature?

The comparison is now added in Section 5.1: relative to the uniform bedrock model (BM07), the realistic basin model amplifies PGA and PGV by ~1.5-2 on average and up to ~3 at the localized western-slope peaks, while the 2D aggravation relative to the matched flat-layer models is ~1.4-2 at these peaks. These values lie within the up-to-fourfold spectral amplification reported for 2D valley resonance (Bard and Bouchon, 1985) and are of the same order as, though lower than, aggravation factors reported for deeper heterogeneous instrumented basins such as the Mygdonian basin (Makra et al., 2005; Raptakis et al., 2005). The up to twofold exceedance of the GMPE predictions has a different reference (the Vs30-based site term) and is not directly comparable to these aggravation factors.

Changes in the manuscript:

> **Section 5.1:** *"Relative to the uniform bedrock model (BM07), the realistic basin model (BM01) amplifies PGA and PGV by a factor of ~1.5-2 on average, rising to ~3 at the localized western-slope peaks, whereas the 2D aggravation relative to the matched flat-layer models amounts to a factor of ~1.5-2 at these peaks. These values lie within the up-to-fourfold spectral amplification reported for 2D valley resonance (Bard and Bouchon, 1985) and are of the same order as, though lower than, aggravation factors reported for deeper, strongly heterogeneous instrumented basins such as the Mygdonian basin (up to 4-6; Makra et al., 2005; Raptakis et al., 2005). The up to twofold exceedance of the GMPE predictions is a separate metric with a different reference (the Vs30-based empirical site term) and is therefore not directly comparable to these aggravation factors."*

Comment 16

Section 4.4.2 – usually for the regressions, slope angle is used on log scale (i.e., use log(slope) for the regressions) since the slope normally has lognormal distribution. Please show the histogram of slope angle and if it is lognormal, try using the log(slope) for the regressions. Could you also show correlation coefficients between different variables used for regressions? Also, with log(slope). Also, check the distribution of PGV, PGA, SSR depth, and SSDS.

The histogram (Figure R1a-b) confirms that the slope-angle distribution is strongly right-skewed and closely lognormal. The log-transformed response variables are closer to normal (Shapiro-Wilk p-values in Figure R1), supporting the logarithmic forms tested in Table S3. Regressions using ln(slope) were indeed tested for all model combinations (Table S3; Figures S9d, S10d/h, S12d/f/g, S13d/f/g) and yield systematically lower R^2 than the untransformed forms (e.g., for SSR: 0.77-0.88 vs. 0.81-0.94); we retain untransformed slope in the featured models because the downslope gravitational shear stress scales with $\sin\theta \approx \theta$ over the observed range (0.2-8.7°). A separate $\sin\theta$ form was not tested because $\sin\theta$ and θ differ by less than 0.4% between 0.2° and 8.7°, so it would yield an essentially identical regression apart from a rescaling of the slope coefficient. All regressions are valid only within the observed data ranges. This reasoning is now revised in Section 3.4.

The correlation matrices (Table R2) now report the correlations between slope angle and the ground motion parameters. Slope angle correlates substantially with the GMPE-derived ground motions (especially in the SSDS dataset). This is physically expected — the GMPE site term depends on Vs30, which in the basin varies systematically with slope angle (steeper slopes carry a thinner, more consolidated sediment cover) — and simply reflects how the ground motions respond to the slope sediments. It does imply, however, that the coefficients of the multivariate GMPE-based regressions should be read as exploratory rather than as calibrated sensitivities. In future work, this interdependence could be reduced by replacing slope angle with a more direct geotechnical measure of the gravitational preconditioning, such as the initial static shear stress acting on the slope sediments, thereby separating the preconditioning term from the Vs30 related site effect on the ground motions. Each regression combines slope angle with a single ground motion parameter (Section 3.4).

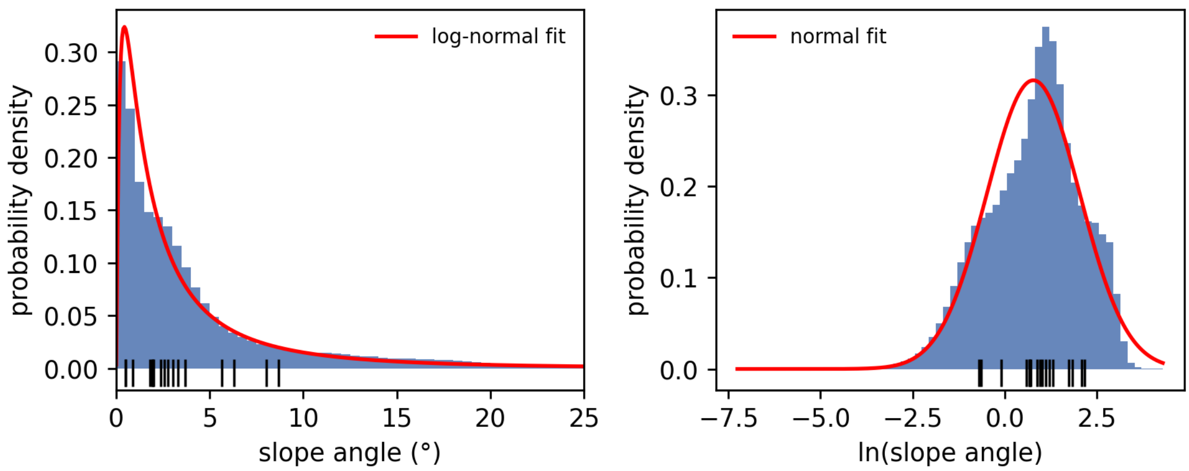

Figure R1. (a) Basin-wide distribution of slope angle derived from the bathymetry, with a fitted log-normal probability density (red); (b) the same data on a natural-log scale with a fitted normal density. Black ticks mark the slope angles at the studied core sites.

Table R2. Correlation coefficients between slope angle and the GMPE-derived ground motion parameters used in the regression analyses (Pearson r, with Spearman ρ in parentheses).

(a) SSR dataset

	PGA	ln(PGA)	PGV	ln(PGV)
slope	0.360 (0.253)	0.383 (0.253)	-0.362 (-0.253)	-0.338 (-0.253)
ln(slope)	0.534 (0.253)	0.563 (0.253)	-0.538 (-0.253)	-0.509 (-0.253)

(b) SSDS dataset

	PGA	ln(PGA)	PGV	ln(PGV)
slope	0.808 (0.764)	0.785 (0.764)	-0.816 (-0.764)	-0.826 (-0.764)
ln(slope)	0.850 (0.764)	0.865 (0.764)	-0.849 (-0.764)	-0.819 (-0.764)

Changes in the manuscript:

Section 3.4: *"For each response variable we tested linear and logarithmic forms of both the response and the predictors, and each regression combines slope angle with a single ground motion parameter. Logarithmic response forms (ln(SSR), ln(SSDS)) avoid non-physical negative predictions for these non-negative quantities, and logarithmic predictor forms (ln(PGA), ln(PGV)) allow for power-law scaling, consistent with the lognormal convention for ground motion parameters Slope angle was retained untransformed in the featured regressions because the downslope gravitational shear stress scales with sin θ ≈ θ over the observed slope range (0.2-8.7°), although ln(slope) forms were also tested (Table S3). The regression variables are slope angle in degrees, PGA in g, PGV in cm s-1, and SSR depth and SSDS thickness in cm; Table S3 compiles all tested forms and their R2 values to show that the sign of the controlling ground motion parameter is robust to the choice of functional form, rather than to select a single best-fitting equation. All regressions are only valid within the observed data ranges."*

Comment 17

Have you compared your event-triggering PGA and PGV values from GMPEs and 2D simulations with the ones from literature? It would be interesting to see the discussion of such a comparison.

The onshore intensities of VII-VIII reported for the 1960 event (Astroza and Lazo, 2008) correspond to ~0.21-0.40 g (Worden et al., 2012). These values cannot be compared directly with our lake-floor estimates: that would assume the same site response onshore and at the lake floor, the assumption this study argues against. What the comparison does show is that the shaking at the lake floor is stronger than the onshore intensities suggest: the 2D simulations locally reach 1-1.5 g, equivalent to ~IX½-X. Intensity thresholds for lacustrine imprints reported in the literature (~V-VI in many regions) are then likely too low if read as lake-floor shaking, and the spread between the GMPE and simulation estimates shows how much progress is still to be made in quantitatively assessing ground motion thresholds for sediment remobilization. Both points are now made in Section 5.3.2.

The SSDS PGA-threshold trend is compatible with the increasing-acceleration thresholds for KHI-related deformation in the Dead Sea (Wetzler et al., 2010; Lu et al., 2020), and the PGV control on SSR is consistent with Wils et al. (2026). The critical acceleration values from geotechnical slope-stability analyses (e.g., Strasser et al., 2007, 2013; ten Brink et al., 2014) are derived from measured geotechnical properties of the slope sediments rather than from GMPE-based shaking estimates, and refer to deeper-seated translational failure generating mass-transport deposits. They are therefore now used as upper-bound references in Section 5.3.1: surficial remobilization is expected to initiate at shaking levels below these failure thresholds. In line with these uncertainties, the exceedance is now phrased as "up to approximately a factor of two" throughout.

Changes in the manuscript:

Section 5.3.2: *"For reference, the macroseismic intensities of VII-VIII reported around the lake for the 1960 event (Astroza and Lazo, 2008) correspond to ~0.21-0.40 g (Worden et al., 2012), of the same order as the GMPE-based estimates at the lake floor (0.24-0.53 g, equivalent to ~VII-VIII½), whereas the 2D simulations locally reach 1-1.5 g, equivalent to ~IX½-X. The shaking at the lake floor can thus be considerably stronger than suggested by the intensities reported onshore. Macroseismic intensity thresholds for lacustrine imprints (~V-VI in many regions; e.g., Monecke et al., 2004; Wilhelm et al., 2016; Kremer et al., 2017; Praet et al., 2017) are based on onshore observations and are likely too low when read as the shaking at the lake floor itself; calibrating such thresholds requires site-specific lake-floor ground motions. The large differences between the GMPE- and simulation-based estimates illustrate how much progress is still to be made in quantitatively assessing ground motion thresholds for sediment remobilization and deformation."*

Section 5.3.1: *"We note that critical acceleration thresholds derived from geotechnical slope-stability analyses (e.g., Strasser et al., 2007; Strasser et al., 2013; ten Brink et al., 2014) address a different process, i.e., deeper-seated translational slope failure generating mass-transport deposits. Because these thresholds are based on measured geotechnical properties and refer to complete slope failure, they can be regarded as upper-bound* *values, the velocity-controlled surficial remobilization considered here is expected to occur at lower shaking levels."*

Comment 18

Discuss the influence of non-linear site response that can be triggered by strong earthquakes like the ones used in the manuscript and possible effects of basin shape on your modelling results (e.g., 2D effects) – how can they alter the ground motion amplitude and frequency content?

We agree that both events impose shear strains capable of driving the soft sediments into the nonlinear regime, which reduces the effective shear modulus (shifting resonance to lower frequencies) and increases hysteretic damping (attenuating high-frequency motion and PGA). The revised manuscript states that the reference simulations are linear visco-elastic (PIMY at its elastic stage, 5% Rayleigh damping at 0.5-10 Hz), retained because this isolates the impedance/geometry effects, because modulus-reduction and damping curves are unmeasured for these diatomaceous sediments, and because the linear solution is a physically meaningful upper bound. New elastoplastic PIMY simulations, now in the Supplement, reduce PGA by ~50-60% in the thick eastern sediments, most strongly for the 1960 event, while the western-slope peaks and the spatial pattern are preserved; the exceedance wording was softened accordingly.

Regarding basin shape and frequency content: surface-to-base transfer functions at three positions (Figure R2) show that each flat-layer model is laterally invariant, but that FM01 and FM02 closely reproduce the spectral response of the basin model at their corresponding positions, with the basin response shifting toward higher frequencies at the thin western slope and toward a lower fundamental frequency at the thick eastern depocenter. The laterally variable spectral content is thus primarily carried by the laterally varying 1D succession of units, which a set of location-matched flat-layer models largely captures, whereas the basin shape itself mainly adds the localized peaks and a moderate aggravation (~1.4-2 at these peaks); a single Vs30 value cannot represent either effect. This hierarchy is now reflected in Sections 5.2 and 6.

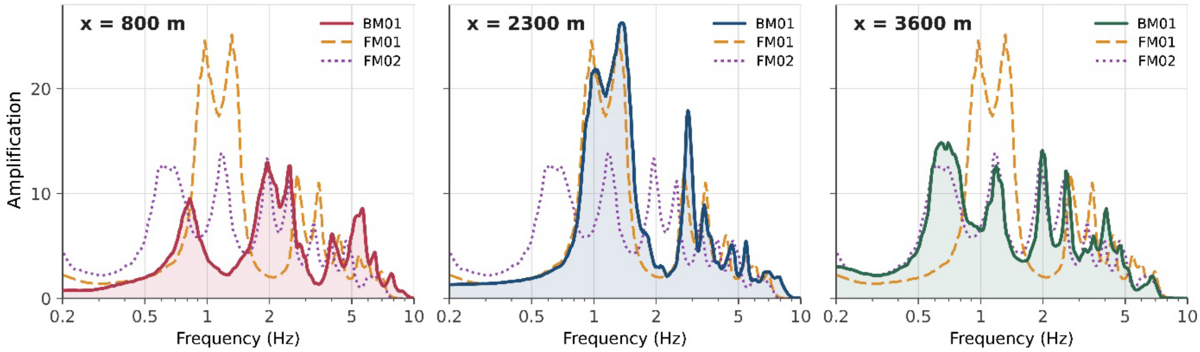

Figure R2. Surface-to-base transfer functions at three positions along the W–E profile: western margin (x = 800 m), towards central basin (x = 2300 m) and central basin (x = 3600 m). Colored solid lines: 2D basin model (BM01); orange dashed and purple dotted lines: flat-layer reference models FM01 and FM02. The flat-layer responses are identical at all positions, whereas the basin response varies along the profile. Transfer functions are from a single representative input motion and are used qualitatively.

Changes in the manuscript:

Section 5.2: "This indicates that the laterally varying succession of units and their impedance contrasts controls the overall amplification level and much of its west-east variation, as matched flat-layer models reproduce the response at the corresponding basin positions, whereas the basin morphology itself mainly adds the localized peaks and a moderate additional aggravation (a factor of ~1.4-2 at these peaks; Section 5.1)."

New Section 5.5 (first paragraph): *"The main simulations assume linear visco-elastic behavior with constant 5% Rayleigh damping (Section 3.3.1). At the shaking levels imposed by the 1960 and 2010 events, the soft lacustrine sediments are expected to respond nonlinearly: modulus reduction shifts the resonance toward lower frequencies, and increased hysteretic damping attenuates high-frequency motion, thereby lowering the PGA amplification (Kramer, 1996). The linear results therefore represent an upper-bound estimate of the amplification. Supplementary sensitivity simulations using the fully elastoplastic PIMY formulation (Figures S14-S15) indicate that nonlinearity reduces PGA by approximately 50-60% in the thick eastern sediments, most strongly for the higher-amplitude 1960 event, while the localized western-slope peaks and the overall west-east amplification pattern are preserved. We therefore consider the spatial pattern of the response robust, whereas the absolute amplitudes, including the up to approximately twofold exceedance of the GMPE predictions, should be interpreted as upper bounds."*

Section 3.3.1: *"In the main analysis, the PIMY materials are kept in their initial, linear elastic stage, and material damping is represented by Rayleigh damping with a target ratio of 5%, anchored at 0.5 and 10 Hz to bracket the basin fundamental frequencies and the dominant input frequencies; the main simulations are thus* *linear visco-elastic, isolating the impedance- and basin-geometry effects that are the focus of this study. The fully nonlinear (elastoplastic) PIMY response is evaluated separately as a sensitivity analysis in the Supplement (Figures S14-S15), and its implications are discussed in Section 5.5."*

Comment 19

Based on your results and "sensitivity analysis" with different "BM" models, can you conclude which components of the model are the most crucial for reliable result – precise velocities? Good stratigraphic/morphological model? Or what? Where should the focus be in case of limited resources for data mining and what can be sacrificed?

We thank the referee for prompting this practically oriented conclusion, now added to the Conclusions. The focus should go into the seismic-stratigraphic survey constraining should go into the seismic-stratigraphic survey constraining the vertical succession of impedance contrasts and its lateral variation across the basin. This stacking controls the amplitude (BM01 to BM03 systematically reduces amplification; BM04 by ~15-25%; BM05 by ~50%, part of which may reflect input coupling, see Comment 14; the uniform BM06 even attenuates) and, through its lateral variation, most of the west-east trend, which location-matched flat-layer models already capture. The specifically two-dimensional contribution of the basin shape consists mainly of localized peaks and a moderate aggravation (~1.4-2); as capturing these peaks reliably would require three-dimensional surveys and models, they are difficult to exploit in practice, which reinforces that the effort should go to the stratigraphy. The precise velocity value per unit is of second-order importance and can be drawn from literature analogues (the alternative-Vp model yields a similar pattern).

Changes in the manuscript:

Section 6 (Conclusion): *"From a practical perspective, the stepwise model comparisons indicate where the effort in future applications should be focused: reliable site-response assessment in lacustrine basins primarily requires seismic-stratigraphic constraints on the basin geometry and on the identity and stacking of the major impedance interfaces, whereas the precise velocity value assigned to each unit is of second-order importance and can be adopted from literature analogues. As the required reflection-seismic data are routinely acquired in lacustrine paleoseismic site surveys, physics-based site-response modeling can be added to such studies at little additional observational cost."*

Comment 20

In Figs. S5-S9, there are fluctuations of amplification on the sides. Is it an artifact due to boundary conditions or how would you explain this?

These are numerical boundary artifacts. At the intersection of the free surface with the lateral dashpot boundaries, the viscous dashpots do not perfectly absorb obliquely incident and surface-wave energy, producing weak spurious waves that decay inward. Unlike the basin models, the flat models were not laterally extended beyond the 4500 m profile, so the artifacts are visible at the profile ends. The laterally uniform response across the central part confirms the interior is uncontaminated, and all FM01/FM02 reference values compared with the basin models and GMPEs were extracted from this central portion, so no result is affected. This is now noted in the captions of Figures S5-S8 (Supplement).

Changes in the manuscript:

Captions of Figures S5-S8: *"Fluctuations near the lateral model edges are numerical boundary artifacts caused by imperfect wave absorption where the free surface meets the lateral dashpot boundaries; all reference values used for comparison were extracted from the central portion of the profile."*

Comment 21

Regressions: please elaborate how you chose the form of the equations and dimensions of predictors and predicted value.

No functional form was assumed a priori. Predictors follow physical mechanisms (slope angle as gravitational preconditioning, PGV for SSR, PGA for SSDS), and each regression combines slope with a single ground motion parameter (Comment 16). For each response we tested linear and logarithmic forms of both response and predictors: log responses avoid non-physical negative predictions for non-negative quantities, and log predictors allow power-law scaling consistent with the lognormal convention for ground motions; slope was kept linear because the driving stress scales with $\sin\theta \approx \theta$ over the observed range, with ln(slope) also tested (a $\sin\theta$ form would be essentially identical, since $\sin\theta$ and θ differ by less than 0.4% over 0.2-8.7°), and all regressions are valid only within the observed data ranges. Units are degrees (slope), g (PGA), cm s-1 (PGV) and cm (SSR/SSDS). Table S3 reports all forms to show the sign of the controlling parameter is robust across forms. This reasoning is now given in Section 3.4 (see the text quoted under Comment 16).

Changes in the manuscript:

Section 3.4: *"For each response variable we tested linear and logarithmic forms of both the response and the predictors, and each regression combines slope angle with a single ground motion parameter. Logarithmic* *response forms (ln(SSR), ln(SSDS)) avoid non-physical negative predictions for these non-negative quantities, and logarithmic predictor forms (ln(PGA), ln(PGV)) allow for power-law scaling, consistent with the lognormal convention for ground motion parameters. Slope angle was retained untransformed in the featured regressions because the downslope gravitational shear stress scales with sin θ ≈ θ over the observed slope range (0.2-8.7°), although ln(slope) forms were also tested (Table S3). The regression variables are slope angle in degrees, PGA in g, PGV in cm s-1, and SSR depth and SSDS thickness in cm; Table S3 compiles all tested forms and their R2 values to show that the sign of the controlling ground motion parameter is robust to the choice of functional form, rather than to select a single best-fitting equation. All regressions are only valid within the observed data ranges."*

Minor comment 1

109-110 "The studied subbasin has no direct river inflows, and therefore sedimentary event deposits can be attributed to seismic triggering." Add references confirming your statement (that it is not a spontaneous failure or human-triggered).

References added. The attribution rests on the absence of river inflows (excluding flood triggering) and on the demonstrated correlation of the event deposits in this basin with historical megathrust earthquakes, which also argues against spontaneous or anthropogenic triggering.

Changes in the manuscript:

Section 2 (Setting): *"The studied subbasin has no direct river inflows, excluding flood-triggered deposition, and the event deposits in this basin have been shown to correlate with historical megathrust earthquakes, so that they can be attributed to seismic triggering (Moernaut et al., 2014; Van Daele et al., 2015; Moernaut et al., 2018; Molenaar et al., 2021)."*

Minor comment 2

119-120 what is the penetration depth of sparker data?

The sparker signal penetrated the complete sedimentary infill, locally up to ~100 m thick, and imaged the acoustic basement along all profiles; this is now stated in Section 3.1.1.

Changes in the manuscript:

Section 3.1.1: *"The sparker data penetrated the entire sedimentary infill (up to ~100 m thick) down to the acoustic basement, with a vertical resolution of about 37–75 cm, while the pinger system provided higher resolution of about 10–20 cm of the upper 15-20 m."*

Minor comment 3

1b: typo in the legend – should be sparker instead of "spaker".

Corrected in Figure 1b.

Minor comment 4

1b, Fig. 5: typo in the legend – should be bathymetry instead of "bathmetry".

Corrected in Figures 1b and 5.

Minor comment 5

1b: label "core locations" is too high with respect to the pink circle.

The label has been repositioned in Figure 1b.

Minor comment 6

1b: it is hard to differentiate the lines showing sparker, pinger, and bathymetry. In B&W, it would be impossible. Consider using lines with different styles (continuous, dashed, ...).

Agreed; the three line types in Figure 1b now use distinct line styles (continuous, dashed and fine line) so that they remain distinguishable in black and white.

Minor comment 7

1b: there is no red line marking the location of the seismic profile shown in Figure 2, as suggested by figure caption.

The profile trace was indeed missing and has been added to Figure 1b.

Minor comment 8

104 – should there be a reference to Fig. 1a instead of 1b?

Correct; the cross-reference has been changed to Figure 1a.

Minor comment 9

108 – typo, "Holcene"

Corrected.

Minor comment 10

Homogenize the use of comma before "and" in the lists.

Comma usage before "and" in lists has been homogenized throughout the revised manuscript.

Minor comment 11

354 – space missing in "from2D". Same for the captions of Figures S5, S6, S7, S8.

Corrected in the captions of Figures 6-7 and S5-S8.

Minor comment 12

358 – "Dashed lines indicate GMPE predictions." – redundancy.

The redundant sentence has been removed from the captions of Figures 6 and 7.

Minor comment 13

8a: Why did you select such steps for the slope angle legend?

The classes were chosen to resolve the low slope-angle range in which all core sites lie (0.5-8.7°; Table S4), at the expense of coarser classes on the steeper slopes not sampled by cores; this is now noted in the caption of Figure 8.

Changes in the manuscript:

> **Caption of Figure 8:** *"Slope-angle classes are refined at low angles to resolve the range covered by the core sites (0.5–8.7°)."*

Minor comment 14

8c-e: please add depth axis for the cores.

Depth axes have been added to the core images in Figures 8c-e and in Figure S4.

References

Astroza, M. and Lazo, R.: Estudio de los daños de los terremotos del 21 y 22 de mayo de 1960, 2008.

Bard, P.-Y. and Bouchon, M.: The two-dimensional resonance of sediment-filled valleys, Bulletin of the Seismological Society of America, 75, 519-541, https://doi.org/10.1785/BSSA0750020519, 1985.

Bertrand, S., Charlet, F., Charlier, B., Renson, V., and Fagel, N.: Climate variability of Southern Chile since the Last Glacial Maximum: a continuous sedimentological record from Lago Puyehue (40°S), Journal of Paleolimnology, 39, 179-195, https://doi.org/10.1007/s10933-007-9117-y, 2008.

BSSC (Building Seismic Safety Council): NEHRP Recommended Provisions for Seismic Regulations for New Buildings and Other Structures (FEMA 450), Federal Emergency Management Agency, Washington, D.C., 2003.

Caiti, A., Akal, T., and Stoll, R. D.: Estimation of shear wave velocity in shallow marine sediments, IEEE Journal of Oceanic Engineering, 19, 58-72, 1994.

Carr, B. J., Hajnal, Z., and Prugger, A.: Shear-wave studies in glacial till, Geophysics, 63, 1273-1284, https://doi.org/10.1190/1.1444429, 1998.

Cressie, N.: The origins of kriging, Mathematical Geology, 22, 239-252, https://doi.org/10.1007/BF00889887, 1990.

Heifetz, E., Agnon, A., and Marco, S.: Soft sediment deformation by Kelvin Helmholtz Instability: A case from

Dead Sea earthquakes, Earth and Planetary Science Letters, 236, 497-504, https://www.sciencedirect.com/science/article/pii/S0012821X05002487, 2005.

Heirman, K.: 'A wind of change': changes in position and intensity of the southern hemisphere westerlies during oxygen isotope stages 3, 2 and 1, http://hdl.handle.net/1854/LU-1900377, 2011.

Kramer, S. L.: Geotechnical Earthquake Engineering, 1996.

Kremer, K., Wirth, S. B., Reusch, A., Fäh, D., Bellwald, B., Anselmetti, F. S., Girardclos, S., and Strasser, M.: Lake-sediment based paleoseismology: Limitations and perspectives from the Swiss Alps, Quaternary Science Reviews, 168, 1-18, https://www.sciencedirect.com/science/article/pii/S0277379117303542, 2017.

Lu, Y., Wetzler, N., Waldmann, N., Agnon, A., Biasi, G. P., and Marco, S.: A 220,000-year-long continuous large earthquake record on a slow-slipping plate boundary, Science Advances, 6, eaba4170, https://doi.org/10.1126/sciadv.aba4170, 2020.

Makra, K., Chávez-García, F. J., Raptakis, D., and Pitilakis, K.: Parametric analysis of the seismic response of a 2D sedimentary valley: implications for code implementations of complex site effects, Soil Dynamics and Earthquake Engineering, 25, 303-315, https://www.sciencedirect.com/science/article/pii/S0267726105000163, 2005.

Moernaut, J., Daele, M. V., Heirman, K., Fontijn, K., Strasser, M., Pino, M., Urrutia, R., and De Batist, M.: Lacustrine turbidites as a tool for quantitative earthquake reconstruction: New evidence for a variable rupture mode in south central Chile, Journal of Geophysical Research: Solid Earth, 119, 1607-1633, https://doi.org/10.1002/2013JB010738, 2014.

Moernaut, J., Van Daele, M., Strasser, M., Clare, M. A., Heirman, K., Viel, M., Cardenas, J., Kilian, R., Ladrón de Guevara, B., Pino, M., Urrutia, R., and De Batist, M.: Lacustrine turbidites produced by surficial slope sediment remobilization: A mechanism for continuous and sensitive turbidite paleoseismic records, Marine Geology, 384, 159-176, http://dx.doi.org/10.1016/j.margeo.2015.10.009, 2017.

Moernaut, J., Van Daele, M., Fontijn, K., Heirman, K., Kempf, P., Pino, M., Valdebenito, G., Urrutia, R., Strasser, M., and De Batist, M.: Larger earthquakes recur more periodically: New insights in the megathrust earthquake cycle from lacustrine turbidite records in south-central Chile, Earth and Planetary Science Letters, 481, 9-19, https://www.sciencedirect.com/science/article/pii/S0012821X17305757, 2018.

Molenaar, A., Van Daele, M., Vandorpe, T., Degenhart, G., De Batist, M., Urrutia, R., Pino, M., Strasser, M., and Moernaut, J.: What controls the remobilization and deformation of surficial sediment by seismic shaking? Linking lacustrine slope stratigraphy to great earthquakes in South-Central Chile, Sedimentology, 68, 2365-2396, https://www.ncbi.nlm.nih.gov/pubmed/34690376, 2021.

Molenaar, A., Van Daele, M., Huang, J.-J. S., Strasser, M., De Batist, M., Pino, M., Urrutia, R., and Moernaut, J.: Disentangling factors controlling earthquake-triggered soft-sediment deformation in lakes, Sedimentary Geology, 438, https://doi.org/10.1016/j.sedgeo.2022.106200, 2022.

Monecke, K., Anselmetti, F. S., Becker, A., Sturm, M., and Giardini, D.: The record of historic earthquakes in lake sediments of Central Switzerland, Tectonophysics, 394, 21-40, https://www.sciencedirect.com/science/article/pii/S0040195104002896, 2004.

Montalva, G. A., Bastías, N., and Rodriguez-Marek, A.: Ground-Motion Prediction Equation for the Chilean Subduction Zone, Bulletin of the Seismological Society of America, 107, 901-911, https://doi.org/10.1785/0120160221, 2017.

Montalva, G. A., Bastías, N., and Leyton, F.: Strong Ground Motion Prediction Model for PGV and Spectral Velocity for the Chilean Subduction Zone, Bulletin of the Seismological Society of America, 112, 348-360, https://doi.org/10.1785/0120210037, 2022.

Oliver, M. A. and Webster, R.: Kriging: a method of interpolation for geographical information systems, International journal of geographical information systems, 4, 313-332, https://doi.org/10.1080/02693799008941549, 1990.

Parla, R. and Somala, S. N.: Seismic Ground Motion Amplification in a 3D Sedimentary Basin: Source Mechanism and Intensity Measures, Journal of Earthquake and Tsunami, 16, 2250008, https://doi.org/10.1142/S1793431122500087, 2022.

Praet, N., Moernaut, J., Van Daele, M., Boes, E., Haeussler, P. J., Strupler, M., Schmidt, S., Loso, M. G., and De Batist, M.: Paleoseismic potential of sublacustrine landslide records in a high-seismicity setting (south-central Alaska), Marine Geology, 384, 103-119, https://www.sciencedirect.com/science/article/pii/S0025322716300767, 2017.

Raptakis, D. G., Manakou, M. V., Chávez-García, F. J., Makra, K. A., and Pitilakis, K. D.: 3D configuration of Mygdonian basin and preliminary estimate of its site response, Soil Dynamics and Earthquake Engineering, 25, 871-887, https://www.sciencedirect.com/science/article/pii/S0267726105001156, 2005.

Shynkarenko, A., Lontsi, A. M., Kremer, K., Bergamo, P., Hobiger, M., Hallo, M., and Fäh, D.: Investigating the subsurface in a shallow water environment using array and single-station ambient vibration techniques, Geophysical Journal International, 227, 1857-1878, https://doi.org/10.1093/gji/ggab314, 2021.

Strasser, M., Stegmann, S., Bussmann, F., Anselmetti, F. S., Rick, B., and Kopf, A.: Quantifying subaqueous slope stability during seismic shaking: Lake Lucerne as model for ocean margins, Marine Geology, 240, 77-97, https://doi.org/10.1016/j.margeo.2007.02.016, 2007.

Strasser, M., Monecke, K., Schnellmann, M., and Anselmetti, F.: Lake sediments as natural seismographs: A compiled record of Late Quaternary earthquakes in Central Switzerland and its implication for Alpine deformation, Sedimentology, 60, 319-341, https://doi.org/10.1111/sed.12003, 2013.

ten Brink, U. S., Chaytor, J. D., Geist, E. L., Brothers, D. S., and Andrews, B. D.: Assessment of tsunami hazard to the U.S. Atlantic margin, Marine Geology, 353, 31-54, https://doi.org/10.1016/j.margeo.2014.02.011, 2014.

Van Daele, M., Moernaut, J., Doom, L., Boes, E., Fontijn, K., Heirman, K., Vandoorne, W., Hebbeln, D., Pino, M., Urrutia, R., Brümmer, R., and De Batist, M.: A comparison of the sedimentary records of the 1960 and 2010 great Chilean earthquakes in 17 lakes: Implications for quantitative lacustrine palaeoseismology, Sedimentology, 62, 1466-1496, https://doi.org/10.1111/sed.12193, 2015.

Van Daele, M., Bertrand, S., Meyer, I., Moernaut, J., Vandoorne, W., Siani, G., Tanghe, N., Ghazoui, Z., Pino, M., Urrutia, R., and De Batist, M.: Late Quaternary evolution of Lago Castor (Chile, 45.6°S): Timing of the deglaciation in northern Patagonia and evolution of the southern westerlies during the last 17 kyr, Quaternary Science Reviews, 133, 130-146, https://doi.org/10.1016/j.quascirev.2015.12.021, 2016.

Wetzler, N., Marco, S., and Heifetz, E.: Quantitative analysis of seismogenic shear-induced turbulence in lake sediments, Geology, 38, 303-306, https://doi.org/10.1130/G30685.1, 2010.

Wiemer, G. and Kopf, A.: Influence of diatom microfossils on sediment shear strength and slope stability, Geochemistry, Geophysics, Geosystems, 18, 333-345, https://doi.org/10.1002/2016GC006568, 2017.

Wiemer, G., Dziadek, R., and Kopf, A.: The enigmatic consolidation of diatomaceous sediment, Marine Geology, 385, 173-184, https://www.sciencedirect.com/science/article/pii/S0025322717300142, 2017.

Wilhelm, B., Nomade, J., Crouzet, C., Litty, C., Sabatier, P., Belle, S., Rolland, Y., Revel, M., Courboulex, F., Arnaud, F., and Anselmetti, F. S.: Quantified sensitivity of small lake sediments to record historic earthquakes: Implications for paleoseismology, Journal of Geophysical Research: Earth Surface, 121, 2-16, https://doi.org/10.1002/2015jf003644, 2016.

Wils, K., Montalva, G., Van Daele, M., De Batist, M., and Moernaut, J.: Peak Ground Velocity and Shaking Duration Control Coseismic Surficial Sediment Remobilization on Lacustrine Slopes and Emplacement of Seismoturbidites, Seismological Research Letters, https://doi.org/10.1785/0220240487, 2026.

Worden, C. B., Gerstenberger, M. C., Rhoades, D. A., and Wald, D. J.: Probabilistic relationships between ground-motion parameters and Modified Mercalli intensity in California, Bulletin of the Seismological Society of America, 102, 204-221, https://doi.org/10.1785/0120110156, 2012.

Yang, Z., Elgamal, A., and Parra, E.: Computational Model for Cyclic Mobility and Associated Shear Deformation, Journal of Geotechnical and Geoenvironmental Engineering, 129, 1119-1127, https://doi.org/10.1061/(ASCE)1090-0241(2003)129:12(1119), 2003.